Chemical Science

ROYAL SOCIETY OF CHEMISTRY

EDGE ARTICLE

View Article Online
View Journal | View Issue

Cite this: *Chem. Sci.*, 2023, **14**, 6688

All publication charges for this article have been paid for by the Royal Society of Chemistry

Received 21st April 2023
Accepted 26th May 2023

DOI: 10.1039/d3sc02076b

rsc.li/chemical-science

Palladium mono-*N*-protected amino acid complexes: experimental validation of the ligand cooperation model in C–H activation†

Sara Fernández-Moyano, Vanesa Salamanca and Ana C. Albéniz *

Mechanistic proposals for the C–H activation reaction enabled by mono-*N*-protected amino acid ligands (MPAAs) have been supported by DFT calculations. The direct experimental observation of the ligand-assisted C–H activation has not yet been reported due to the lack of well-defined isolated palladium complexes with MPAAs that can serve as models. In this work, palladium complexes bearing chelating MPAAs $(NBu_4)[Pd(\kappa^2\text{-}N,O\text{–AcN–CHR–COO})(C_6F_5)py]$ (Ac = MeC(O); R = H, Me) and $[Pd(\kappa^2\text{-}N,O\text{–MeNH–}CH_2\text{–COO})(C_6F_5)py]$ have been isolated and characterized. Their evolution in a solution containing toluene leads to the C–H activation of the arene and the formation of the C_6F_5–C_6H_4Me coupling products. This process takes place only for the ligands with an acyl protecting group, showing the cooperating role of this group in a complex with a chelating MPAA, therefore experimentally validating this working model. The carboxylate group is inefficient in this C–H activation.

Introduction

Mono-*N*-protected amino acids (MPAAs) are extremely important ligands in palladium catalyzed C–H functionalization reactions.[1] Yu's group introduced them in 2008 and they showed that these ligands strongly accelerated coupling reactions that involved a C–H activation.[2] They also demonstrated the utility of these ligands in enantioselective C–H functionalization.[2–4] Since then, MPAAs have been used in a myriad of transformations of $C(sp^3)$–H and $C(sp^2)$–H bonds and they are one of the most important types of cooperating ligands in these reactions.[5,6]

MPAAs usually conform to the formulation PGNH-backbone-COOH where PG = acyl group. The presence of several donor atoms of moderate coordination ability makes MPAAs potential polydentate ligands that can act in a mono and dianionic forms. Therefore, different coordination modes to the metal are possible, which complicate the study of these systems, but this is important in the metal speciation in a catalytic process. Possible binding modes are: monodentate $(\kappa^1\text{-}O)^-$ (X ligand), chelating $(\kappa^2\text{-}N,O)^-$ (XL ligand), chelating $(\kappa^2\text{-}N,O)^{2-}$ (X_2 ligand) and bridging $(\mu^2\text{-}O,O)^-$ (μ-XL ligand), the latter leading to polynuclear complexes (Scheme 1).

The role of MPAAs in catalytic C–H functionalization can be manifold and these ligands can be involved in the stabilization of intermediates or in other steps of the catalysis different from the C–H cleavage.[7,8] However their main role is to facilitate the C–H activation step and the importance of the presence of the acyl monoprotection to enable this process was early recognized.[2,5b] This protecting group exerts a cooperating role in the C–H cleavage *via* the involvement of the acyl oxygen in a concerted metalation deprotonation (CMD) mechanism. It has been proposed that the MPAA is coordinated to palladium in a chelating dianionic $(\kappa^2\text{-}N,O)^{2-}$ form,[1c,9] and the transfer of the C–H hydrogen to the acyl oxygen occurs in the transition state, transforming the dianionic MPAA into a monoanionic ligand (Scheme 2(a)).[10] This working model also explains the asymmetric induction observed in enantioselective C–H functionalization,[11] and it is commonly proposed with the support of computational studies.[12] However, the situation can be more complex and it is worth noting that calculations have also supported that the C–H activation in a MPAA–Pd mononuclear complex can be assisted by an external base such as acetate or carbonate (outer sphere CMD) and, in fact, the energy difference between both pathways can be small.[13] In addition, just the

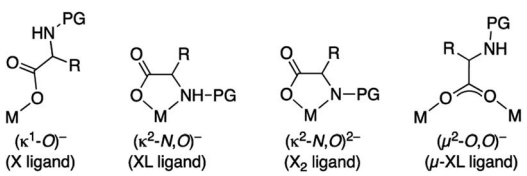

Scheme 1 Coordination modes of mono-*N*-protected amino acids.

IU CINQUIMA/Química Inorgánica, Universidad de Valladolid, 47071-Valladolid, Spain. E-mail: albeniz@uva.es

† Electronic supplementary information (ESI) available: Experimental details, characterization data, crystal XRD and computational details. CCDC 2255463–2255465, 2255468 and 2255469. For ESI and crystallographic data in CIF or other electronic format see DOI: https://doi.org/10.1039/d3sc02076b

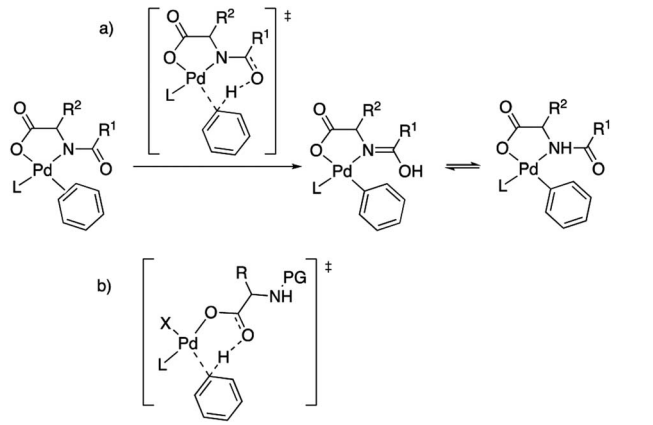

Scheme 2 Models for MPAA cooperation in C–H activation: (a) chelating model with assistance of the acyl protecting group; (b) carboxylate assistance with no involvement of the protecting group.

carboxylate moiety in the MPAA can assist the C–H activation with no involvement of the protecting group as found in some computational studies (Scheme 2(b)).[14] Dinuclear rather than mononuclear palladium complexes have been proposed as relevant species in the C–H activation step and, in the reported example, calculations show that a bridging $(\mu^2\text{-}O,O)^-$ MPAA is present but the amino acid is not directly involved in the C–H cleavage, which is assisted by an additional coordinated acetate.[15] For C–H functionalizations that use silver bases, the formation of heterometallic Pd–Ag species has been suggested based on DFT calculations. In this case a CMD process is assisted by the MPAA carboxylate moiety as shown in Scheme 2(b).[14]

Mechanistic studies on some C–H functionalization reactions enabled by MPAAs, usually alkenylation reactions of arenes, have inferred the formation of mononuclear MPAA–palladium species during catalysis by kinetic experiments,[16] mass spectrometry studies,[10,11a,12b,17] and diffusion NMR spectroscopy.[12b] However, the actual C–H activation step has never been modeled experimentally. The analysis of the optimal Pd/MPAA ratio for the acceleration of a C–H functionalization reaction has been analyzed as an indication of the nuclearity of the catalytic species in the C–H cleavage step. This analysis can be complicated by the fact that, because MPAAs can significantly lower the barrier for C–H activation, other steps in the catalytic cycle can become turnover limiting. In some cases, MPAAs can have a detrimental effect on other steps in the catalytic cycle and this has been shown by Stahl *et al.*[18] Thus, the optimal Pd/MPAA ratio can be the result of a compromise between opposing effects of the ligand during the catalytic cycle and it may not reflect the actual composition of the C–H activation transition state. The experimental validation of the proposed model for C–H activation enabled by MPAAs requires the observation of this step in a system where the coordination mode of the amino acid is well-stablished and the role of the MPAA in the C–H cleavage can be separated from the influence of other additives (bases, OAc^-, *etc.*). We describe here the synthesis of well-defined palladium complexes with chelating MPAAs and we show that they react with arenes *via* C–H activation. By comparing acyl and methyl protecting groups, it is possible to unequivocally show the ability of acyl-MPAAs to induce the C–H cleavage *via* metal–ligand cooperation.

Results and discussion

Palladium complexes with a chelating *N*-acetylglycine (**2**) and *N*-acetylvaline (**3**) were prepared by reaction of $(NBu_4)[PdBr_2(C_6F_5)py]$ (**1**) and the corresponding amino acid ligand in the presence of silver carbonate as shown in eqn (1). Both complexes bear a pentafluorophenyl group that allowed us to monitor the C–H activation reactions by detecting the coupling products C_6F_5–aryl (see below). This strategy has proved useful in our former studies on the role of cooperating bipyridone ligands in C–H activation.[19] The presence of a fluorinated tag is also very useful in the characterization of the species formed. Pyridine, a ligand of moderate coordination ability, completes the coordination sphere of palladium and imparts enough stability to the complexes without blocking further reactivity by ligand substitution.

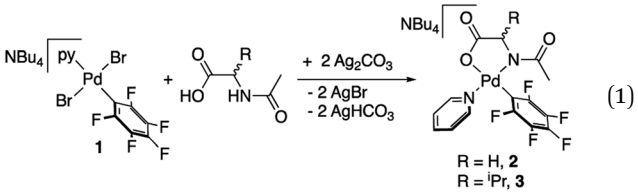

(1)

Complexes **2** and **3** were characterized by NMR, elemental analyses and mass spectrometry. The MPAA ligand is coordinated in a chelating dianionic $(\kappa^2\text{-}N,O)^{2-}$ form. A ^1H–^{19}F HOESY NMR experiment shows a cross peak between the methyl substituent of the acetyl group and the F_{ortho} of the perfluoroaryl indicating, therefore, that they are close to each other in space (see Fig. S30 and S35, in the ESI†). This experiment confirms the coordination of the nitrogen of the amino acid to palladium and unequivocally determines the stereochemistry of the complexes. In addition, no dissociation of the pyridine ligand was observed in solution and the complexes are monomeric as shown by ^{19}F NMR DOSY experiments (see Section 1.6, ESI†). We could not obtain crystals suitable for X-ray diffraction and attempts at crystallization of complex **2** only led to the ligand reorganization and the formation of the bis MPAA complex **4** and the bis-aryl **5** that crystallized out (eqn (2)). The molecular structures of these complexes are shown in Fig. 1.[20] This reorganization is slow at temperatures equal or below 298 K and the formation of **4** and **5** occurs after keeping layered solutions of **2** for long periods of time.

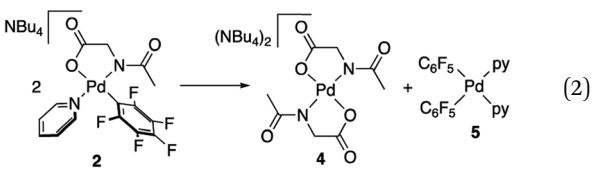

(2)

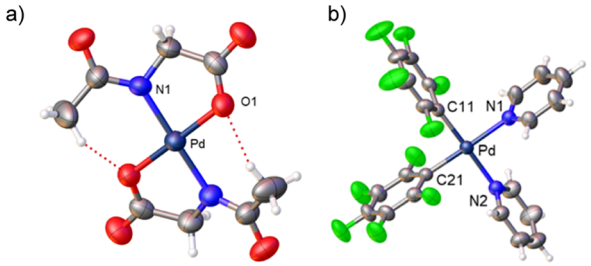

Fig. 1 X-ray molecular structure of complexes **4** ((a) NBu_4^+ omitted for clarity) and **5** (b) (ORTEP, 40% probability). Selected bond lengths (Å): **4**, Pd–N(1) = 2.018(3), Pd–O(1) = 2.002(3); **5**, Pd–N(1) = 2.104(3); Pd–N(2) = 2.104(3); Pd–C(11) = 1.994(3); Pd–C(21) = 1.994(3).

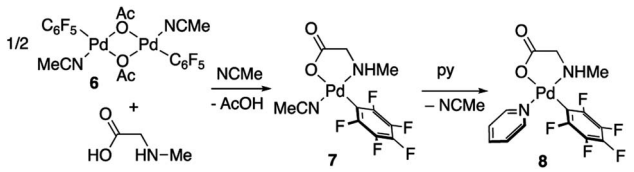

Scheme 3 Synthesis of complexes **7** and **8**.

Derivatives of *N*-methylglycine (sarcosine) were also prepared. In this case the alternative synthetic route depicted in Scheme 3 was used. The amino acid is acting as a chelating monoanionic $(\kappa^2\text{-}N,O)^-$ ligand in complexes **7** and **8**. The less acidic NH moiety in sarcosine does not deprotonate even when carbonate is used as a base. In fact, the synthetic route depicted in eqn (1) only gives complex **8** when sarcosine is used albeit in lower yield than that in the procedure shown in Scheme 3. Complexes **7** and **8** were completely characterized and Fig. 2 shows the molecular structure of complex **8** (see Fig. S16† for complex **7**).[20] It is noteworthy that both derivatives are monomeric showing the higher preference of the monoanionic amino acid ligand to bind in a chelating fashion rather than a dimeric form with a bridging $(\mu^2\text{-}O,O)^-$ coordination mode.

With these complexes at hand we tested their ability to enable the C–H activation process by heating them up in the presence of an arene and in the absence of other reagents (Table 1). When the *N*-acetylglycine derivative **2** was heated either in toluene or in ethylbenzoate at 130 °C the C–H functionalization of the arene was observed and the biaryl coupling products C_6F_5–C_6H_4R (R = Me, COOEt) were formed as major decomposition products in 30 min (entries 1 and 2, Table 1).

Complex **2** is very stable in pyridine and the product of the C–H arylation of this arene is only observed as a minor product (entry 3, Table 1). The C–H functionalization of toluene occurs when the arene is used as reactant and solvent as well as in a mixture of the arene and a cosolvent such as DMA (entries 1 and 4, Table 1). HFIP was also tested and the coupling products were observed, albeit in lower amount (entry 9). The C–H activation products were obtained as a mixture of regioisomers, the *meta* substitution being the predominant one (Table S1, ESI†). Pentafluorobenzene and aryl reorganization complexes bearing the "$Pd(C_6F_5)_2$" moiety were also observed as byproducts. The formation of bispentafluorophenyl complexes most probably occurs by transmetalation of C_6F_5 groups from one Pd to another as observed and studied before.[21]

The C–H functionalization occurs for the acyl protected amino acid complexes **2** and **3**, whereas it is inefficient for the methyl protected sarcosine derivative **8** (*cf.* entries 5–7, Table 1). This experimentally shows the feasibility of the chelating model of assistance of the C–H activation with the direct involvement of the acyl group. It also shows that the presence of the amino acid carboxylate moiety is not enough for an efficient C–H cleavage (entry 7, Table 1).

The reaction of complex **2** in a mixture of toluene/DMA was monitored by ^{19}F NMR at 90 °C. Fig. 3 shows the course of the reaction. In addition to the toluene C–H functionalization products and a small amount of C_6F_5H, a new organometallic product (**9**) was formed (eqn (3)). This complex was also observed when the decomposition was carried out at 130 °C for short reaction times (Fig. 4 and entry 4, Table 1).

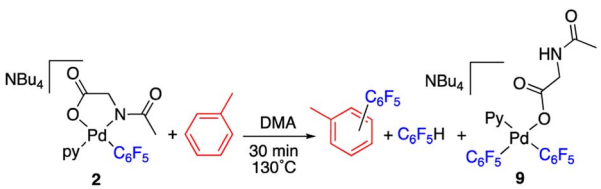

(3)

Complex **9** shows the characteristic NMR pattern of a "$Pd(C_6F_5)_2$" moiety where both aryls are chemically inequivalent. After thorough experimentation, **9** could be identified as a palladium derivative with a monodentate $(\kappa^1\text{-}O)^-$ amino acid ligand. This derivative was independently synthesized as shown in Scheme 4 and it is a rare example of this coordination mode for a MPAA ligand.[22] Complex **9** was characterized by NMR and its formulation and monomeric nature was confirmed by DOSY experiments (Section 1.6, ESI†).

The decomposition of complex **9** occurs slowly in toluene/DMA at 130 °C to give the biaryl coupling product and C_6F_5H, the latter in a higher relative molar amount than that observed for complex **2** (entry 8, Table 1 and Fig. S4†). This product distribution is consistent with the reaction pathway shown in Scheme 5. First, the protonation of one of the

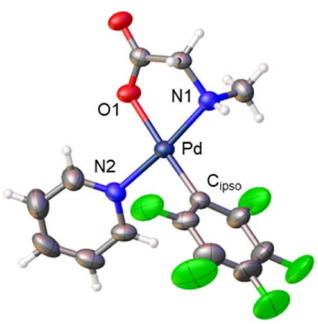

Fig. 2 X-ray molecular structure of complex **8** (ORTEP, 40% probability). Selected bond lengths (Å): Pd–O(1) = 2.065(3); Pd–N(1) = 2.045(3); Pd–N(2) = 2.039(3); Pd–C_{ipso} = 1.995(5).

Table 1 Decomposition products of MPAA-complexes when heated in the presence of an arene[a]

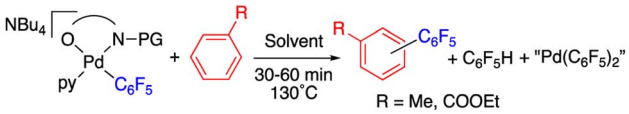

Entry	Complex	Solvent	Time	Conversion, %	C_6F_5–arene, %	C_6F_5H, %	"$Pd(C_6F_5)_2$",[b] %
1	**2**	Toluene	30 min	82	53	17	—[c]
2	**2**	PhCOOEt	30 min	100	83	17	—
3	**2**	Pyridine	30 min	10	6	—	4 ($[Pd(C_6F_5)_2py_2]$)
4	**2**	Toluene/DMA (1 : 1)	30 min	100	75	12	13 (**9**)
5	**2**	Toluene/DMA (1 : 1)	60 min	100	79	21	—
6	**3**	Toluene/DMA (1 : 1)	60 min	100	77	23	—
7	**8**	Toluene/DMA (1 : 1)	60 min	38	10	5	23 ($[Pd(C_6F_5)_2py_2]$)
8	**9**	Toluene/DMA (1 : 1)	60 min	42	16	26	—
9[d]	**2**	Toluene/HFIP (1 : 1)	60 min	100	31	27	5 (C_6F_5–C_6F_5)[c]

[a] Reaction temperature: 130 °C. The percentages shown correspond to the mol% of fluorinated compounds and they were determined by integration of ^{19}F NMR signals. [b] Pd-species formed in parenthesis. [c] Other unidentified Pd–C_6F_5 complexes account for the remaining 12% in entry 1 and 37% in entry 9. [d] Reaction temperature: 90 °C due to the low boiling point of HFIP.

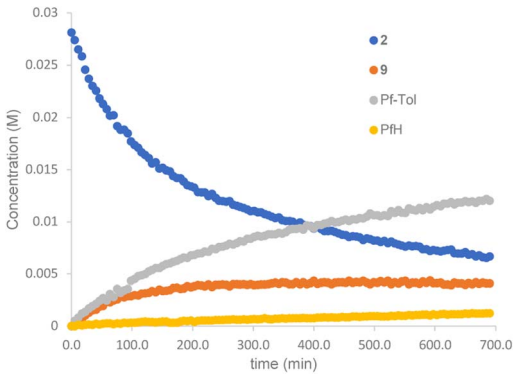

Fig. 3 ^{19}F NMR follow up of the decomposition of complex **2** in a mixture of toluene/DMA at 90 °C (Pf = C_6F_5).

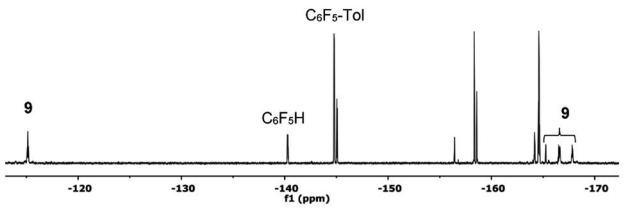

Fig. 4 ^{19}F NMR spectrum (470.17 MHz) of the product mixture obtained after heating complex **2** at 130 °C in toluene/DMA (1/1) for 30 min (entry 4, Table 1). Only the F_{ortho} region for the organic products has been labelled for clarity.

pentafluorophenyl groups of the complex takes place and this could occur by the amino acid acting as a hydrogen donor. This process leads to the formation of complex **2** that is responsible for the C–H activation of toluene.

The reaction of complex **2** in toluene was modelled by DFT calculations using the M06 functional and including solvation in the optimizations through the SMD implicit solvent method (see the ESI† for details). The reaction profile for the formation of C_6F_5–C_6H_4–*m*-Me is represented in Fig. 5 and the resulting energy barriers are consistent with the experimental conditions needed for the decomposition of **2**. The C–H activation of toluene assisted by the MPAA requires the *cis* arrangement of the coordinated arene and amido fragment of the amino acid ligand (intermediate **c1**). In the case of complex **2** this requires a *cis–trans* isomerization and a rotation of the acyl group around

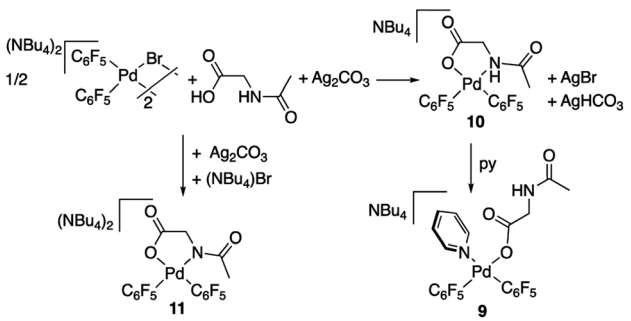

Scheme 4 Synthesis of bis-pentafluorophenyl palladium complexes with the *N*-acetylglycine ligand.

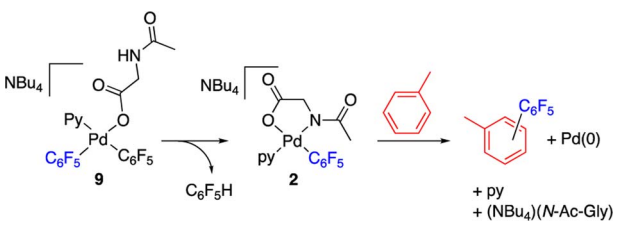

Scheme 5 Plausible decomposition route of complex **9** *via* C–H activation.

the C–N bond. The energy difference between complex **2** and the isomer closest to the required stereochemistry (**2b$_{rot}$**) is not high (less than 5 kcal mol^{-1}) and the calculated barrier for rotation about the C(acyl)–N bond of the amino acid is 18.6 kcal mol^{-1}, much lower than the barrier for C–H activation (see Fig. S56, ESI†). Therefore, at the temperature needed for the decomposition of the complex, both processes are expected to be faster than the subsequent C–H cleavage. The overall barrier for the C–H activation from **2** is 29.2 kcal mol^{-1} and it is determined by a CMD transition state with the assistance of the acyl oxygen. The formation of the coupling product follows, by reductive elimination of the pentafluorophenyl and the tolyl groups. This process is very energy demanding as expected for the perfluorinated aryl group and, in fact, the reductive elimination step shows the higher energy barrier in the calculated reaction profile. The measured kinetic isotope effect, determined in separate experiments, has a low value, KIE = 1.4 ± 0.1, and it is consistent with a scenario where the C–H cleavage is not controlling the reaction rate and there is a subsequent step of higher energy barrier. Since the C–H activation precedes this step a measurable but small KIE may be observed derived from the different equilibrium concentrations of **c2**.[23] The barriers for reductive elimination are much lower for non-polyfluorinated aryls,[19b,24] and, therefore, in these cases the C–H activation step is expected to be the one with highest energy barrier.‡ It has to be noted that, by itself, the low KIE value observed does not rule out other possibilities such as the existence of a previous step close in energy to the C–H activation, or an electrophilic metalation pathway for the C–H activation (secondary KIE by rehybridization). Nonetheless, the latter is less likely for the anionic electron rich complexes involved in these reactions.

The palladium complexes with coordinated *N*-acetylglycinates **9–11** depicted in Scheme 4 show some interesting features regarding the coordination modes of this ligand. The protonated nitrogen atom of the monoanionic *N*-acetylglycinate is a weak donor and complex **10** shows a fluxional behavior in solution consistent with the fast decoordination–recoordination of this atom. The ^{19}F NMR spectrum of **10** shows broad signals at room temperature and equivalent pentafluorophenyl groups, which indicate a fast *cis–trans* isomerization and nitrogen inversion. This process could occur: (i) *via* dissociation of the NHAc group, topomerization and recoordination or (ii) *via* an associative NHAc substitution by the carboxylate and formation of intermediate carboxylato-bridged dimeric species (Scheme 6). The mass spectrum of **10** shows the monomeric complex depicted in Schemes 4 and 6 as the predominant species ($[Pd(C_6F_5)_2(AcNH–CH_2COO)]^-$, *m*/*z* 555.9168) but it also shows a minor fragment of molecular weight corresponding to $[\{Pd(C_6F_5)_2\}_2(AcNH–CH_2COO)]^-$ (*m*/*z* 995.8060) indicating that the formation of dimeric species is also possible. Unfortunately, complex **10** is not stable in solution long enough to perform additional DOSY experiments. Therefore, the occurrence of dimeric species as reaction intermediates for the protonated monoanionic *N*-acetylglycinato cannot be ruled out. Musaev, Lewis *et al.* have reported the synthesis of dimeric species for analogous monoanionic MPAAs, where the complex bears a metalated benzylamine fragment.[25] This precedent and the results here show that the $(\kappa^2\text{-}N,O)^-$ and bridging $(\mu^2\text{-}O,O)^-$ coordination modes for monoanionic MPAA ligands are close in energy and the adoption or one or the other can be determined by the additional ligands completing the coordination sphere of palladium. In our case, the monomeric species **10** are more stable than the dimeric situation by 2.7 kcal mol^{-1} as shown by DFT calculations. The presence of equimolar amounts of pyridine leads to complex **9** (Scheme 4) showing that the use of an additional ligand in C–H functionalization reactions (dual-ligand enabled reactions),[6e,26] may ensure the formation of monomeric species throughout the C–H activation process: dianionic $(\kappa^2\text{-}N,O)^{2-}$ before C–H activation (exemplified by complex **2**) and monoanionic $(\kappa^1\text{-}O)^-$ after C–H activation (as in complex **9**). Complex **11** (Scheme 4) was also synthesized and it shows a static behavior with well-defined ^{19}F NMR signals corresponding to the two inequivalent pentafluorophenyl rings.

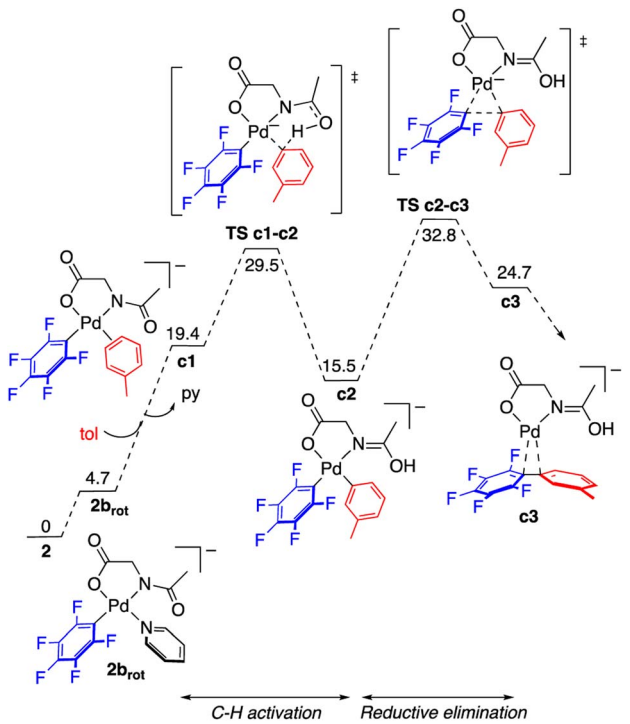

Fig. 5 Gibbs energy profile for the formation of the C–H functionalization product $C_6F_5–C_6H_4–m$-Me from complex **2** in toluene at 130 °C (energies in kcal mol^{-1}).

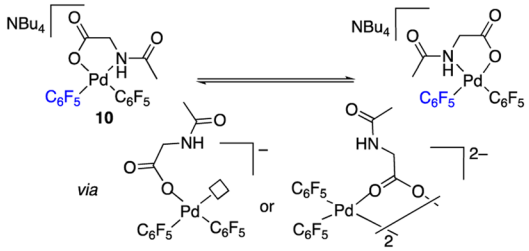

Scheme 6 Fluxional behavior of complex **10**.

The much better donor amido AcN moiety leads to the preferred chelating coordination mode of the dianionic *N*-acetylglycinate.

Conclusions

We have experimentally shown that the C–H activation of a simple arene (toluene) occurs on a palladium complex bearing a chelating dianionic acyl-monoprotected amino acid $(\kappa^2\text{-}N,O)^{2-}$ in the absence of any external base, consistent with previously reported computational findings. The presence of the acyl group is necessary for the C–H activation and the acyl oxygen is involved in the CMD transition state. This gives the strongest support to the current working model for these reactions: the occurrence of an intermediate palladium complex with a chelating MPAA responsible of the C–H activation as well as the enantioselection. The carboxylato moiety in the ligand, a potential assisting group, has no significant participation in the C–H cleavage as shown by the inefficiency of the analogous methyl protected amino acid ligand (sarcosine derivative) to bring about the C–H activation of toluene. The complexes prepared show how monoprotected amino acids bind, leading to palladium monomeric complexes: dianionic chelating bidentate, monoanionic chelating bidentate and monoanionic monodentate binding modes are preferred. Our results do not support the formation of dimeric carboxylate-bridging complexes as predominant species for these ligands in the complexes studied, although in the case of monoanionic MPAA ligands they may exist as short-lived reaction intermediates. It must be noted that the nature of the ligands that complete the coordination sphere of palladium, other than the MPAA (substrate, additional auxiliary ligands, *etc.*), will have a strong influence in determining the preferred coordination mode of the monoanionic MPAAs during catalysis. The dianionic MPAAs bind in a chelating bidentate mode as expected for the strong deprotonated AcN donor group.

Data availability

Data supporting this article have been uploaded as ESI.†

Author contributions

S. F. M. and V. S. conducted the investigation under A. C. A. supervision. A. C. A. wrote the manuscript and S. F. M. prepared the ESI.† All authors contributed to the conceptualization of the project and the review and editing of the manuscript.

Conflicts of interest

There are no conflicts to declare.

Acknowledgements

We acknowledge the financial support of the Spanish MICINN (AEI, PID2019-111406GB-I00) and the Junta de Castilla y León-FEDER (VA224P20), as well as the joint support of the EU/MICINN/JCyL (C17.I01.P01.S21, H_2MetAmo).

Notes and references

‡ Although the reductive elimination is the plausible step right after the C–H cleavage, other processes such as ligand tautomerization in the conditions herein (absence of an added base) or a change in coordination mode of the ligand to $(\kappa^1\text{-}O)^-$ by pyridine coordination cannot be ruled out.

1 (*a*) K. M. Engle, *Pure Appl. Chem.*, 2016, **88**, 119–138; (*b*) D. Wang, A. B. Weinstein, P. B. White and S. S. Stahl, *Chem. Rev.*, 2018, **118**, 2636–2679; (*c*) Q. Shao, K. Wu, Z. Zhuang, S. Qian and J. Q. Yu, *Acc. Chem. Res.*, 2020, **53**, 833–851; (*d*) S. K. Sinha, S. Guin, S. Maiti, J. P. Biswas, S. Porey and D. Maiti, *Chem. Rev.*, 2022, **122**, 5682–5841.

2 B. F. Shi, N. Maugel, Y. H. Zhang and J. Q. Yu, *Angew. Chem., Int. Ed.*, 2008, **47**, 4882–4886.

3 B. F. Shi, Y. H. Zhang, J. K. Lam, D. H. Wang and J. Q. Yu, *J. Am. Chem. Soc.*, 2010, **132**, 460–461.

4 Pioneering proof of concept work that showed the ability of chiral aminoacids to induce enantioselective C–H activation: V. I. Sokolov, L. L. Troitskaya and O. A. Reutov, *J. Organomet. Chem.*, 1979, **182**, 537–546.

5 Early work: (*a*) D.-H. Wang, K. M. Engle, B.-F. Shi and J.-Q. Yu, *Science*, 2010, **327**, 315–319; (*b*) K. M. Engle, D. H. Wang and J. Q. Yu, *J. Am. Chem. Soc.*, 2010, **132**, 14137–14151; (*c*) K. M. Engle, D. H. Wang and J. Q. Yu, *Angew. Chem., Int. Ed.*, 2010, **49**, 6169–6173; (*d*) K. M. Engle, P. S. Thuy-Boun, M. Dang and J. Q. Yu, *J. Am. Chem. Soc.*, 2011, **133**, 18183–18193.

6 Some recent examples of MPAA-enabled reactions. Olefination: (*a*) T. K. Achar, X. Zhang, R. Mondal, M. S. Shanavas, S. Maiti, S. Maity, N. Pal, R. S. Paton and D. Maiti, *Angew. Chem., Int. Ed.*, 2019, **58**, 10353–10360; (*b*) Q. J. Yao, P. P. Xie, Y. J. Wu, Y. L. Feng, M. Y. Teng, X. Hong and B. F. Shi, *J. Am. Chem. Soc.*, 2020, **142**, 18266–18276; (*c*) J. Das, T. Pal, W. Ali, S. R. Sahoo and D. Maiti, *ACS Catal.*, 2022, **12**, 11169–11176; (*d*) Z. Fan, X. Chen, K. Tanaka, H. S. Park, N. Y. S. Lam, J. J. Wong, K. N. Houk and J.-Q. Yu, *Nature*, 2022, **610**, 87–93; Cyanation: (*e*) H. Chen, A. Mondal, P. Wedi and M. Van Gemmeren, *ACS Catal.*, 2019, **9**, 1979–1984; Carbonylation: (*f*) X. F. Bai, Q. C. Mu, Z. Xu, K. F. Yang, L. Li, Z. J. Zheng, C. G. Xia and L. W. Xu, *ACS Catal.*, 2019, **9**, 1431–1436; Thiolation: (*g*) S. K. Sinha, S. Panja, J. Grover, P. S. Hazra, S. Pandit, Y. Bairagi, X. Zhang and D. Maiti, *J. Am. Chem. Soc.*, 2022, **144**, 12032–12042, C–H/C–H cross coupling: (*h*) Z.-J. Cai, C.-X. Liu, Q. Gu, C. Zheng and S.-L. You, *Angew. Chem., Int. Ed.*, 2019, **58**, 2149–2153, Arylation: (*i*) P. Dolui, J. Das, H. B. Chandrashekar, S. S. Anjana and D. Maiti, *Angew. Chem., Int. Ed.*, 2019, **58**, 13773–13777; C–H addition to alkenes: (*j*) J. Das, P. Dolui, W. Ali, J. P. Biswas, H. B. Chandrashekar, G. Prakash and D. Maiti, *Chem. Sci.*, 2020, **11**, 9697–9702.

7 R. E. Plata, D. E. Hill, B. E. Haines, D. G. Musaev, L. Chu, D. P. Hickey, M. S. Sigman, J. Q. Yu and D. G. Blackmond, *J. Am. Chem. Soc.*, 2017, **139**, 9238–9245.

8 X. Cong, H. Tang, C. Wu and X. Zeng, *Organometallics*, 2013, **32**, 6565–6575.

9 (*a*) D. G. Musaev, A. Kaledin, B.-F. Shi and J. Q. Yu, *J. Am. Chem. Soc.*, 2012, **134**, 1690–1698; (*b*) D. G. Musaev, T. M. Figg and A. Kaledin, *Chem. Soc. Rev.*, 2014, **43**, 5009–5031.

10 G. J. Cheng, Y. F. Yang, P. Liu, P. Chen, T. Y. Sun, G. Li, X. Zhang, K. N. Houk, J. Q. Yu and Y. D. Wu, *J. Am. Chem. Soc.*, 2014, **136**, 894–897.

11 (*a*) G. J. Cheng, P. Chen, T. Y. Sun, X. Zhang, J. Q. Yu and Y. D. Wu, *Chem.–Eur. J.*, 2015, **21**, 11180–11188; (*b*) B. E. Haines, J. Q. Yu and D. G. Musaev, *ACS Catal.*, 2017, **7**, 4344–4354; (*c*) T. G. Saint-Denis, R. Y. Zhu, G. Chen, Q. F. Wu and J. Q. Yu, *Science*, 2018, **359**, eaao4798.

12 (*a*) X. M. Zhong, G. J. Cheng, P. Chen, X. Zhang and Y. D. Wu, *Org. Lett.*, 2016, **18**, 5240–5243; (*b*) P. Wedi, M. Farizyan, K. Bergander, C. Mück-Lichtenfeld and M. Gemmeren, *Angew. Chem., Int. Ed.*, 2021, **60**, 15641–15649; (*c*) K. Mukherjee, N. Grimblat, S. Sau, K. Ghosh, M. Shankar, V. Gandon and A. K. Sahoo, *Chem. Sci.*, 2021, **12**, 14863–14870; (*d*) L. P. Xu, Z. Zhuang, S. Qian, J. Q. Yu and D. G. Musaev, *ACS Catal.*, 2022, **12**, 4848–4858.

13 B. E. Haines and D. G. Musaev, *ACS Catal.*, 2015, **5**, 830–840.

14 L. Fang, T. G. Saint-Denis, B. L. H. Taylor, S. Ahlquist, K. Hong, S. Liu, L. Han, K. N. Houk and J. Q. Yu, *J. Am. Chem. Soc.*, 2017, **139**, 10702–10714.

15 J. J. Gair, B. E. Haines, A. S. Filatov, D. G. Musaev and J. C. Lewis, *ACS Catal.*, 2019, **9**, 11386–11397.

16 D. E. Hill, K. L. Bay, Y. F. Yang, R. E. Plata, R. Takise, K. N. Houk, J. Q. Yu and D. G. Blackmond, *J. Am. Chem. Soc.*, 2017, **139**, 18500–18503.

17 R. Jayarajan, J. Das, S. Bag, R. Chowdhury and D. Maiti, *Angew. Chem., Int. Ed.*, 2018, **57**, 7659–7663.

18 C. A. Salazar, J. J. Gair, K. N. Flesch, I. A. Guzei, J. C. Lewis and S. S. Stahl, *Angew. Chem., Int. Ed.*, 2020, **59**, 10873–10877.

19 (*a*) V. Salamanca, A. Toledo and A. C. Albéniz, *J. Am. Chem. Soc.*, 2018, **140**, 17851–17856; (*b*) V. Salamanca and A. C. Albéniz, *Org. Chem. Front.*, 2021, **8**, 1941–1951; (*c*) C. Pinilla, V. Salamanca, A. Lledós and A. C. Albéniz, *ACS Catal.*, 2022, **12**, 14527–14532.

20 Deposition numbers 2255463 (for **1**), 2255464 (for **4**), 2255465 (for **5**), 2255468 (for **7**), and 2255469 (for **8**) contain the crystallographic data for this paper.†

21 (*a*) A. L. Casado, J. A. Casares and P. Espinet, *Organometallics*, 1997, **16**, 5730–5736; (*b*) A. C. Albéniz, P. Espinet, O. López-Cimas and B. Martín-Ruiz, *Chem.–Eur. J.*, 2005, **11**, 242–252.

22 This coordination mode has been proposed in reactions of *N*-acetyl glycine in water: T. G. Appleton, D. R. Bedgood and J. R. Hall, *Inorg. Chem.*, 1994, **33**, 3834–3841.

23 E. M. Simmons and J. F. Hartwig, *Angew. Chem., Int. Ed.*, 2012, **51**, 3066–3072.

24 (*a*) E. Clot, C. Mégret, O. Eisenstein and R. N. Perutz, *J. Am. Chem. Soc.*, 2009, **131**, 7817–7827; (*b*) E. Gioria, J. delPozo, J. M. Martínez-Ilarduya and P. Espinet, *Angew. Chem., Int. Ed.*, 2016, **55**, 13276–13280.

25 J. J. Gair, B. E. Haines, A. S. Filatov, D. G. Musaev and J. C. Lewis, *Chem. Sci.*, 2017, **8**, 5746–5756.

26 (*a*) H. Chen, P. Wedi, T. Meuer, G. Tavakoli and M. van Gemmeren, *Angew. Chem., Int. Ed.*, 2018, **57**, 2497–2501; (*b*) D. Zhao, P. Xu and T. Ritter, *Chem*, 2019, **5**, 97–107.